

1 **A study on the performance of low-cost sensors for source**
2 **apportionment at an urban background site**

3
4 **Dimitrios Bousiotis¹, David C.S. Beddows¹, Ajit Singh¹, Molly Haugen²,**
5 **Sebastián Diez³, Pete M. Edwards³, Adam Boies², Roy M. Harrison¹, and**
6 **Francis D. Pope^{1*}**

7
8 ¹Division of Environmental Health and Risk Management, School of Geography, Earth and
9 Environmental Sciences University of Birmingham, Edgbaston, Birmingham B15 2TT,
10 United Kingdom

11
12 ²Department of Engineering, University of Cambridge, Trumpington Street, Cambridge,
13 CB2 1PZ, United Kingdom

14
15 ³Wolfson Atmospheric Chemistry Laboratories, Department of Chemistry, University of
16 York, Heslington, York YO10 5DD, United Kingdom

17
18 *Corresponding Author, correspondence to Francis Pope f.pope@bham.ac.uk

19 **Abstract**

20 Knowledge of air pollution sources is important in policy making and air pollution mitigation.
21 Until recently, source apportion analyses were limited and only possible with the use of
22 expensive regulatory-grade instruments. In the present study we applied a two-step Positive
23 Matrix Factorisation (PMF) receptor analysis at a background site in Birmingham, UK using
24 data acquired by low-cost sensors (LCS). The application of PMF allowed for the
25 identification of the sources that affect the local air quality, clearly separating different
26 sources of particulate matter (PM) pollution. Furthermore, the method allowed for the
27 contribution of different air pollution sources to the overall air quality at the site to be
28 estimated, thereby providing pollution source apportionment. The use of data from
29 regulatory-grade (RG) instruments further confirmed the reliability of the results, as well as
30 further clarifying the particulate matter composition and origin. Comparing the results from
31 a previous analysis, in which a k-means clustering algorithm was used, a good consistency
32 between the k-means and PMF results was found in pinpointing and separating the sources
33 of pollution that affect the site. The potential and limitations of each method when used
34 with low-cost sensor data are highlighted. The analysis presented in this study paves the
35 way for more extensive use of LCS for atmospheric applications, receptor modelling and
36 source apportionment. Here, we present the infrastructure for understanding the factors
37 that affect air quality at a significantly lower cost than previously possible. This should
38 provide new opportunities for regulatory and indicative monitoring for both scientific and
39 industrial applications.

40 **1. Introduction**

41 Air pollution is a major problem not only affecting human health (Pascal et al., 2013; Rivas
42 et al., 2021; Shiraiwa et al., 2017; Wu et al., 2016; Zeger et al., 2008), but also causing
43 environmental deterioration and social disparity due to its effect on climate change
44 (Manisalidis et al., 2020; Mannucci and Franchini, 2017; Moore, 2009). Air pollution is
45 typically more problematic in urban environments which have multiple air pollution sources,
46 or locations near pollution hot spots (Valavanidis et al., 2008, Bousiotis et al., 2021). The
47 knowledge of air pollution sources is vital in understanding the air quality at a given site as
48 well as for policy making and action to improve air quality. Such knowledge was provided,
49 until recently, by the analysis of data from expensive regulatory grade (RG) instruments. The
50 use of RG instruments was not extensive due to their high cost and bulky size limiting their
51 use almost exclusively for scientific research. As a result, there is limited knowledge of the
52 sources that affect the air quality. This is in part due to the small number of deployments
53 and hence low spatial resolution of these expensive instruments (Kanaroglou et al., 2005),
54 especially in low- and middle-income countries. In these areas the problem of air quality and
55 its effect on human health is of great importance and expected to further increase in the
56 coming years as a result of their rapid industrial and population growth (Kan et al., 2009;
57 Petkova et al., 2013). To combat this, in the past decade, the development of low cost
58 sensors (LCS) measuring either PM or gas phase pollutant concentrations has intensified
59 (Lewis et al., 2018; Penza, 2019; Popoola et al., 2018). These LCS are still far from being an
60 equal alternatives to the more expensive RG instruments. Many limitations are associated
61 with their use, with the main shortcoming being the inconsistency of their measurements,
62 even for similar sensors deployed at the same site (Austin et al., 2015; Sousan et al., 2016),
63 either due to operational and detector sacrifices that allow them to be inexpensive or from
64 the effect of meteorological conditions that affect their measurements (Crilley et al., 2020;
65 Hagan and Kroll, 2020; Wang et al., 2021). Thus, consistent calibration (Kosmopoulos et al.,
66 2020; De Vito et al., 2020) and data corrections (Crilley et al., 2018; Liang et al., 2021; Vajs et
67 al., 2021) are required for these sensors to provide reliable measurements, although
68 sometimes even this is not enough (Giordano et al., 2021). Nevertheless, these sensors have
69 the potential to change the state of air pollution monitoring by allowing wider use and
70 better spatio-temporal coverage.

71 Many applications of LCS have been found in recent years at sites that were previously
72 inaccessible by regulatory instrumentation, either due to them being cost prohibitive
73 (Miskell et al., 2018; Omokungbe et al., 2020; Pope et al., 2018), or due to their physical size
74 limitations (Jovašević-Stojanović et al., 2015; Nagendra et al., 2019, Whitty et al., 2022).
75 Additionally, the use of LCS made possible higher spatial resolution measurements than RG
76 instruments (Feinberg et al., 2019; Krause et al., 2019; Prakash et al., 2021). Thereby greatly
77 improving the ability to measure air quality at multiple locations of interest, even down to
78 the neighbourhood scale (Schneider et al., 2017; Shafran-Nathan et al., 2019; Shindler,
79 2021). LCS have been shown to help supplement existing regulatory networks (Weissert et
80 al., 2020). While the applications of LCS provided the information of the level of air quality
81 at more sites, vital information on air pollution sources and the environmental conditions
82 that enable or inhibit air pollution, as well as their relative contributions is yet to be
83 exploited by LCS data. Pope et al., (2018) using PM ratios, managed to separate and identify
84 the effect of major sources of pollution in several cities in East Africa LCS data. Popoola et al,
85 (2018) identified the sources of pollution near Heathrow Airport, London using a network of
86 LCS. Bousiotis et al., (2021) using k-means clustering on PM data from both a LCS and an RG
87 instrument, showed the strengths and limitations of the sensor, in measuring particle
88 number concentrations and using them to identify the sources of pollution at a background
89 site in Birmingham, UK. While these studies identified many sources and conditions that
90 affect air quality, they provided no information on their temporal variability and the relative
91 contributions of different sources.

92 In the present study, a two-step PMF technique proposed by Beddows and Harrison (2019),
93 an advanced version of a statistical method for source apportionment successfully applied
94 in many studies with RG instruments (Beddows et al., 2015; Harrison et al., 2011; Hopke,
95 2016; Leoni et al., 2018; Pokorná et al., 2016), is applied on data collected from various LCS.
96 This provides a quantitative separation of the different sources and their contributions to a
97 background site located in Birmingham. Furthermore, data from RG instruments and an
98 Aerosol Chemical Speciation Monitor (ACSM) were used to provide further nuance to the
99 analysis. This was done not only to compare the results from the two sets, but to further
100 characterise the sources of larger sized particles at the site as well. The results of the
101 present analysis are also compared with those from a previous study at the same site made
102 by Bousiotis et al., (2021) using k-means clustering, displaying the additional information

103 provided by the PMF as well as to check the consistency of the results between the two
104 methods. To the authors' knowledge source apportionment with LCS data has only been
105 attempted previously by Hagan et al., (2019) using Non-negative Matrix Factorisation (a
106 derivative version of PMF in which all components of the data matrix are weighted equally
107 rather than with individual errors) on a dataset from New Delhi, India. This study provided
108 information about combustion and non-combustion air pollution sources as well as their
109 partial contributions in a three-factor solution. The present work prepares the ground for
110 future use of source apportionment with LCS in a variety of scientific and industrial
111 scenarios. This will make more feasible their wider use, either as standalone air pollution
112 sources data sources, or in combination with RG instruments for increasing spatial coverage.
113

114 **2. Methods**

115 **2.1 Location of the site and instruments**

116 The measurement site is the Birmingham Air Quality Supersite (BAQS) located at the
117 grounds of the University of Birmingham (52.45°N; 1.93°W) (fig. 1). This is an urban
118 background site within a large residential area about 3 km southwest of the city centre of
119 Birmingham. For this site, PM concentration measurements in the range 0.35 to 40 μm were
120 collected using an Alphasense OPC-N3 in a 10 second resolution (averaged in 1-hour
121 resolution) for the period between 16/10/2020 to 30/10/2020. Additionally, data from
122 several LCS were also collected. NO, NO₂ and ozone measurements were collected using the
123 Box Of Clustered Sensors (BOCS, Smith et al., 2019) in the same time resolution, as well as
124 black carbon (BC) concentrations using the MA200 sensor by Magee Scientific. Finally, the
125 data for the lung deposited surface area (LDSA) of particles in the range of 10 nm to 10 μm ,
126 which is found to strongly correlate with BC emissions (Lepistö et al., 2022), was collected
127 using a set of two Naneos Partectors by Naneos Particle Solutions GmbH. One sensor
128 measured the surface of all particles in this size range, while the second is placed after a
129 catalytic stripper (Catalytic Instruments CS015) which removes the semi-volatile particles
130 (Haugen et al. 2022).

131 Apart from the data provided directly from the sensor before the catalytic stripper, the ratio
132 between the measurements of the two Naneos Partectors was also considered according to:
133

134
$$LDSA_{ratio} = \frac{LDSA \text{ after the catalytic stripper}}{LDSA \text{ before the catalytic stripper}}$$

135

136 This was done to resolve whether such a configuration can provide additional information
137 for the origin of pollution or the age of the pollutants in the incoming air masses, as
138 increased concentrations of semi-volatile compounds are usually associated with
139 anthropogenic sources, especially in the urban environment (Mahbub et al., 2011, Schnelle-
140 Kreis et al., 2007, Xu and Zhang, 2011). Thus, a high $LDSA_{ratio}$ is expected to be associated
141 with fresher pollution which usually has a higher content of volatile compounds (i.e.,
142 pollution sources at a close distance from the site), while lower ratios are probably
143 associated with either cleaner conditions or more regional and aged pollution with higher
144 concentrations of semi-volatile compounds, generally associated with sources at a greater
145 distance from the measuring site. This specific metric was also used in our previous study
146 (Bousiotis et al., 2021) and the consistency of the results between the two will be
147 compared.

148 For better characterisation of the larger particles, the Aerodyne ACSM was used, providing
149 information about its composition in the size range between 40 nm to 1 μm for NO_3^- , SO_4^{2-}
150 and organic content. For the comparison of the results, data from RG instruments were also
151 used, namely a Palas FIDAS (for PM), a Teledyne T500U (for NO_x), a Thermo 49i (for O_3) and
152 an AE33 aethalometer from Magee Scientific (for BC). Comparison of the regulatory
153 instruments and the LCS allows for consistency of the results between instrument types to
154 be checked. A detailed description of the operation and more information about the sensors
155 and instruments used in this study can be found in Bousiotis et al., (2021).

156

157

158 **2.2 Positive Matrix Factorisation and data analysis**

159 The PMF is a multivariate data analysis, developed by Paatero (Paatero and Tapper, 1993;
160 1994), which is the most commonly used method for source apportionment and has been
161 applied numerous times in the field of aerosol science. The method is a weighted least-
162 squares technique that describes relationships among species measurements (Reff et al.,
163 2007). It assumes that X is a matrix of observed data, typically either particle number size

164 distributions (PNSDs) or chemical composition data, and u is the known matrix of the
165 experimental uncertainty of X . Both X and u are of dimensions $n \times m$ (where n is the number
166 of measurements and m is the number of species measured). The method solves the
167 bilinear matrix problem $X = GF + E$ where F is the unknown right hand factor matrix
168 (sources) of dimensions $p \times m$, G is the unknown left hand factor matrix (contributions) of
169 dimensions $n \times p$, and E is the matrix of residuals. The problem is solved in the weighted
170 least-squares sense: G and F are determined so that the Euclidean norm of E divided
171 (element-by-element) by u is minimized. Furthermore, the solution is constrained so that all
172 the elements of G and F are required to be non-negative (Paatero and Tapper, 1994). Higher
173 F values account for better association of the given variable with the factor it is assigned to,
174 while higher G values account for greater contribution of the factor at the given time period.

175 In the present analysis, a combination of both PNSD and particle composition data were
176 used. Such a combination may cause several shortcomings in the application of the PMF as
177 different types of data are used, due to the significant difference between the nature of
178 each variable. While this could be overcome by increasing the total weights of the primary
179 group of measurements (the one considered better in driving the model), this could be
180 problematic in the treatment and importance of the auxiliary dataset in the model
181 (Beddows and Harrison, 2019). To overcome these shortcomings the two-step PMF method,
182 proposed by Beddows and Harrison (2019), was used. In the first step of the method, a part
183 of the dataset is PMF-analysed (i.e. composition) and a solution is provided. The time series
184 G values (and errors) of the solution from the first step are then used as input variables to
185 the second step, where they are combined with the additional measurements (i.e. PNSD
186 data) dataset applying a second PMF analysis (a flow diagram of the method used as
187 presented by Beddows and Harrison, 2019 is found in figure S1). In the present study the
188 opposite path was considered, with the first step using the PNSD provided by the OPC
189 sensor and the inclusion of particle composition data in the second step. This was explicitly
190 done for two reasons: 1. to test the capabilities of the LCS in source apportionment, 2. to
191 connect specific PNSD profiles with specific pollution sources. Furthermore, on the second
192 step of the analysis detailed in Beddows and Harrison (2019) the explained variance of the
193 factors from the first step were maximised. This directly connects the additional variables in
194 the second step with the PNSD profiles found in the first step, excluding the possible factors

195 formed with the data from the additional LCS data. In the present study, this step in this
196 method was omitted, as the aim is to present the results of the receptor model as they
197 occur in real life using a combination of LCSs measuring both particle number
198 concentrations and composition.

199 As PMF is a descriptive model there is no objective criterion in the choice of the optimal
200 number of factors (Paatero et al., 2002). In all cases several solutions were tested, and the
201 solution chosen was the one that provided factors with unique properties. Solutions with
202 additional factors provided no extra information on additional sources, rather the additional
203 factors separated factors that had already found into smaller groups with no significant
204 covariation.

205 For the study site, particle number concentration data were available from the OPC for
206 particles of diameter $< 40 \mu\text{m}$, but only data up to $10 \mu\text{m}$ were used. This was due to the
207 lack of sufficient non-zero counts in the larger size bins above that size threshold, which
208 disfavours PMF analysis to be completed. Additionally, separate LCS data for NO and NO₂
209 were available from the BOCS. The NO data showed sensible variation (which is the more
210 important factor in the PMF analysis), however, a great number of the NO data points had
211 low negative values due to their very low concentrations, which is impossible data for the
212 PMF algorithm. Rather than removing the negative numbers or artificially calibrating the
213 data upwards, we use NO_x (NO + NO₂) as the variable of interest.

214 Finally, to avoid the increased uncertainties from the use of unavailable data (as missing
215 data are treated with increased uncertainties), a time window for which all data were
216 available was chosen. Thus, data availability is 100% and no special treatment was
217 considered for missing data.

218 Finally, for the present study the PMF analysis was performed using the second iteration of
219 the PMF software developed by Paatero (2004a; 2004b). Data was analysed using the
220 Openair package for R (Carlslaw and Ropkins, 2012), and back trajectory data were
221 extracted by NOAA Air Resources Laboratory and calculated using the HYSPLIT model
222 (Draxler and Hess, 1998).

223

224

225 **3. Results**

226 **3.1 General conditions at the BAQS site and overall performance of the low-** 227 **cost sensors**

228 The measuring period (16th to 30th of October 2020) was chosen as it is a period which
229 presented rather typical meteorological conditions in the area, had no missing data from
230 any of the instruments used, and because they were the last days before the second
231 lockdown due to COVID-19 was applied (31st of October 2020). General meteorological
232 conditions were rather typical for the period in Birmingham, UK. As a result, the conditions
233 and activities in the surrounding area found in this period are considered almost consistent
234 with the normal conditions at the site in the autumn season. Mean temperature was $10.0 \pm$
235 2.5°C and mean relative humidity was $87.9 \pm 7.5 \%$ (standard deviations are calculated using
236 hourly data) during the measurement period. The average wind profile (Fig. S2) was also
237 typical for the UK with mainly southwestern winds of relatively low speed ($2.1 \pm 1.1 \text{ m s}^{-1}$).

238
239 Most of the LCS correlated well when compared to their more expensive RG counterparts,
240 using the Pearson correlation coefficient as the measure of correlation. The OPC-N3
241 presented a strong correlation for PM_1 ($r = 0.88$), though its performance weakened with
242 greater sized PM ($r = 0.49$ for $\text{PM}_{2.5}$ and $r = 0.46$ for PM_{10}). The decreasing correlation from
243 PM_1 to $\text{PM}_{2.5}$ to PM_{10} is likely due to greater wall losses in the tubing for the bigger particles.
244 Strong correlations were also found from the BOCS sensors as well, with both O_3 and NO_x
245 concentrations presenting high r values when compared with their respective RG
246 instrument measurements (0.95 and 0.82 respectively). Finally, the BC measuring LCS
247 presented lower agreement with the measurements from the RG instrument, with a
248 Pearson correlation value of 0.40. It is noted, in the present study the absolute performance
249 of the LCS is not of great importance and thus it is not analysed in depth. For the PMF model
250 to present meaningful results the representation of the relative values and variability of the
251 variables is crucial instead, and this is thoroughly tested in the present study.”

252 253 **3.2 First step PMF analysis (PNSD analysis)**

254 Following the discussed methodology a 4-factor solution was chosen for this analysis. The
255 PNSD profiles of the factors found are presented in Figure S3. Due to the limited variation of

256 the PNSD profiles when presenting all the size bins available, making some of them appear
257 identical (i.e. Factor 2 and 3, due to the increasing particle number concentration as the size
258 decreases), the smallest particle diameter size bin at 400 nm (particle diameter range
259 between 350 to 460 nm) was removed to better present the variation on the larger sizes.
260 Thus, the particle profiles without the smallest available size are presented in Figure 2. The
261 profiles in the range between 500 nm to 10 μm for the four factors, associated with unique
262 formations extracted from the method are:

- 263 • Factor 1, that presents no significant peaks in the measured range of the OPC, but
264 does show a steady increasing trend with particle diameters below 1 μm
- 265 • Factor 2, with a distinct particle diameter peak at about 2 μm
- 266 • Factor 3, with a distinct particle diameter peak at about 2 μm and an increasing
267 trend below 750 nm
- 268 • Factor 4, accounting for particle diameter peaking at about 750 nm and 1.5 μm .

269

270 **3.3 Second step PMF with LCS data (LC analysis)**

271 The four-factor solution was also chosen in the second step analysis, for which the results of
272 the first step are combined with the additional particle and gas phase composition datasets
273 from LCS. The addition of more factors instead of adding information or providing clearer
274 associations with the factors from the first step, it separated the existing factors and their
275 association with the particle composition data into mixed factor groups with less significant
276 contributions of the variables. The association of the variables with each factor is presented
277 in figure 3, while the temporal variation of the contributions G of all the factors from this
278 analysis is presented in figure 4, along with the wind profile for some periods when each
279 factor was dominant.

280

281 The four new factors are:

282 **LC1 (Local and city centre pollution on calm conditions):** The LC1 is strongly associated with
283 the first factor from the initial PMF on the PNSD. For the period when the contribution of
284 this factor is higher (18th and 19th of October, see fig. 4) rather slow winds prevail from
285 many sectors (in this case mainly from the southwest). This factor has higher contributions
286 during calm conditions and during periods with north-eastern winds, though with lower

287 contribution (Fig. 5). It is highlighted that at the northeast of the specific site is the city
288 centre of Birmingham which is one of the main sources of pollution as found from a
289 previous study (Bousiotis et al., 2021). Looking at the diurnal variation (Fig. S4) of this factor
290 we see increased contributions during early morning and evening hours, likely associating it
291 with the morning and evening rush hours. The increased contributions during night-time
292 should not be overlooked and are probably the result of the lower boundary layer height
293 (BLH) during this time of the day. Additional data analysis shows an increased association of
294 this factor with PM_{10} (Fig. 3), though this association is reduced for particles of larger sizes,
295 further confirming the lack of additional peaks on greater sizes. This along with the
296 increased association with the LDSA indicates the presence of large number of particles
297 below the detection limit of the instrument. This factor is also associated with almost all the
298 pollutants used, such as NO_x , CO and BC, though not as strongly as factor LC3 that is
299 discussed below, probably associated with pollution sources in a closer range to the
300 measuring station, as well as to a smaller extent with pollution from the city centre. Its
301 connection with air masses from the northeast is also confirmed from the back trajectory
302 analysis (Fig. 6), in which the highest contributions of this factor were found for air masses
303 from the northeast.

304 **LC2 (Marine):** This factor is strongly associated with the fourth PNSD factor from the initial
305 analysis (fig. 3). It presents relatively high association with PM which increases as the size
306 increases. No other significant association is found rather than relatively weak ones with
307 ozone, CO and the $LDSA_{ratio}$. It does not have a clear diurnal variation (fig. S4), though it has
308 slightly increased contributions during night-time. Higher contributions for this factor are
309 found with south and south-eastern winds of high speed (fig. 4 and 5). This can be seen in
310 Figure 4, where the highest contributions of this factor are associated with strong southern
311 winds. The marine nature of this factor is clearly highlighted through the back trajectory
312 analysis for this factor (Fig. 6) in which higher contributions are mostly found with air
313 masses originating from the north Atlantic Ocean, while some contributions from southern
314 Spain and Africa, which may be associated with Saharan dust and pollution from these
315 areas.

316 **LC3 (midday city centre and southwest pollution):** This factor does not have any significant
317 association with any of the factors from the PMF analysis of the PNSD (fig. 3). It presents
318 greater contributions during the midday (fig. S4), and it is associated with north-eastern and

319 southwestern winds (fig. 5). It has high contributions with all the pollutants included in the
320 analysis and the $LDSA_{ratio}$, which points to fresher pollution (pollution sources closer to the
321 measuring station). Such sources of pollution in most cases are associated with particles of
322 sizes smaller than that measured by the OPC, hence the lack of association with any of the
323 factors found from the PNSD analysis. The back trajectory analysis provides no clear origin
324 for the air masses of this factor (fig. 6), which may indicate a relatively smaller pollution
325 lifetime, which is associated with incoming air masses from all directions.

326 **LC4 (Urban background)**: This factor has a rather strong association with the second factor
327 from the PNSD analysis and a weaker one with the third one (Fig. 3). It does not have a clear
328 diurnal variation (fig. S4) and it is mainly associated with north-eastern winds (Fig. 5). It
329 presents weak associations with all the variables inputted in the PMF analysis making it hard
330 to distinguish either a source or conditions for which this factor is enhanced. The back
331 trajectory analysis though shows that this factor is associated with air masses from
332 continental Europe as well as Scandinavia (Fig. 6), which for the UK, usually contain aged
333 and hence typically larger secondary PM pollutants.

334

335 **3.4 Second step PMF with RG data (RG analysis)**

336 While the primary aim of the present study is to highlight the capabilities of LCS in source
337 apportionment, the measurements provided by these devices are mainly focused on gas
338 phase pollutants which are in most cases associated solely with ultrafine particles. The OPC
339 measurements used for this site have a particle diameter range between 400 nm to 10 μm .
340 Thus, apart from using data from RG instruments measuring gas phase pollutants, it was
341 considered sensible to add data from an ACSM, which measures compounds associated with
342 larger particles, such as nitrate, sulphate, and organic compounds (used in this analysis).
343 Some of the factors in this analysis are rather similar with those formed from the analysis
344 using LCS dataset. Thus, the **RG1** factor in this analysis is mainly associated with the first
345 factor from the PNSD analysis in the first step (Fig. 7), similar to that found also in LC1 (Fig.
346 3). The wind conditions are also similar for which these factors from the two analyses
347 present their highest contribution (Fig. 8), as well as their temporal variation (Fig. S5) and
348 diurnal variation (Fig. S6). The additional information granted using the ACSM data is the
349 strong association of this factor with nitrate, and a stronger association with NO_x and BC are

350 also found, compared to the LC analysis. This further associates this factor with nearby
351 sources of pollution which prevail with low wind speeds and may associate the conditions of
352 this factor with the low BLH height found during that time, though high contributions were
353 also found for early morning and evening hours, as in the LC analysis for the similar factor.
354 Finally, the back trajectory analysis (fig. 9) shows higher contributions associated with air
355 masses from the northeast, further confirming its similarity with the first factor from the LC
356 analysis and its urban origins.

357 The **RG2** is unique and has no association with the factors from the PMF on PNSD data and
358 is strongly associated only with sulphate (Fig. 7). It does not have a clear diurnal variation
359 (fig. S6) and seems to have higher contributions with southwestern winds of rather high
360 speed and to a lesser extent with north-easterly winds (Fig. 8). The back trajectory analysis
361 (Fig. 9), while presenting few relatively high contributions from continental Europe, mainly
362 associates this factor with incoming air masses from all sea origins surrounding the UK. This
363 is expected as the ocean is a source of sulphate containing compounds (for the particles at
364 the size range measured by the OPC), either sea-salt sulphate or marine biogenic sulphate
365 (Lin et al., 2012; Raes et al., 2000).

366 The **RG3** is similar to the LC2 and is mainly associated with the fourth factor from the PNSD
367 analysis and to a lesser extent with the third (Fig. 7). This factor has slightly increased
368 contributions during night-time (Fig. S6) and south and southwestern winds (Fig. 8). It
369 presents increased associations with increasing PM size, though in this case it is also
370 strongly associated with O₃. Unfortunately, no Cl or Na data were available to further
371 determine the marine nature of this factor. The back trajectory analysis though once again
372 presents higher contributions with marine air masses (Fig. 9), though some hot spots are
373 also found from continental Europe, which probably explain to an extent the small
374 associations found with NO_x and organic compounds from the ACSM.

375 Finally, the **RG4** is mainly associated with the second factor and to a lesser extent with the
376 third from the PNSD analysis (Fig. 7). It presents higher contributions with north-eastern
377 winds (Fig. 8), has an unclear diurnal variation (Fig. S6), and presents higher contributions
378 with air masses from continental Europe (Fig. 9), like the LC4 from the second-step analysis.
379 While in that analysis it was difficult to characterise the sources for that factor, the strong
380 association with organic compounds found here with the addition of the ACSM data helps in
381 its clearer characterisation.

382

383 **4. Discussion**

384 **4.1 Comparison of the results from the second-step analysis**

385 It should be noted that regardless of any possible similarities between the two (second-
386 step) analyses, a direct comparison of the results should be conducted with great care. As
387 different variables are considered, even minor differences may result in different trends,
388 contribution of variables and the sources described. Regardless, the results of the two
389 analyses have great similarities especially on specific factors that are associated with the
390 same particle size distribution profiles (from the PNSD analysis), contribution of chemical
391 compounds and diurnal variation. Three factors were found to have great similarities and
392 were associated with similar particle profiles. Specifically, these are the factors describing
393 the sources of particles which are either in close proximity to the measuring station or occur
394 with almost calm conditions (Factor 1 on both analyses), the marine factor (Factor 2 on LC
395 analysis and 3 on RG analysis) and the continental factor (Factor 4 on both analyses).
396 Looking at their temporal contributions (Fig. 4 and S5), the first factors on both analyses
397 appear to consistently peak on periods when the second set of factors (LC2 and RG3)
398 presents lower G contributions (and vice versa), which is expected due to the nature of their
399 sources. The factors on both sets though have almost identical temporal variation of their G
400 contributions regardless of the dataset. For the fourth factors on both analyses, though
401 presenting similar associations with their variables, differences are found in their temporal
402 variations with the addition of the ACSM data. This shows that while these factors appear to
403 be almost identical, small differences can still be found in their temporal variation and
404 variable associations, when different datasets are considered. Nevertheless, the addition of
405 the ACSM data shows a very high contribution of NO_3^- on the first RG factor, SO_4^{2-} for the
406 second factor and the organic component on the fourth factor.
407 The remaining factor from both analyses though is completely different between the two
408 analyses and point towards the differences on the variables used for each. In the LC analysis
409 the factor formed consists of sources that are associated with fresher pollution sources.
410 Thus, a factor with strong associations with all the pollutants available was formed, it was
411 not associated with any of the PNSD formations from the first-step analysis and presented a
412 unique diurnal variation peaking midday. This should be expected as the particle size

413 measured by the OPC is much larger compared to the size of the particles these chemical
414 compounds are usually associated with. The occurrence of this factor was probably included
415 partially to the first and fourth factor of the RG analysis, as these present relatively higher
416 associations with NO_x and BC and more enhanced contributions during midday hours
417 compared to their LC analysis counterparts.

418 Finally, using the RG instrument data, the additional factor is associated with sulphate
419 alone. This is a result that was consistent regardless of the number of factors used, either
420 greater or smaller. Sulphate containing compounds have a lower volatility compared to the
421 other chemical compounds used in the analysis and is relatively more stable with a rather
422 small seasonal variation (Utsunomiya and Wakamatsu, 1996), thus having a longer lifespan
423 and distance of travel. As a result, sulphate was found not to be associated with any other
424 chemical compound and always formed a factor of its own (regardless of the number of
425 factors chosen).

426

427 **4.2 Comparison with the results from a previous study.**

428 Although different methodologies were used with the previous analysis for the BAQS site
429 (Bousiotis et al., 2021), as well as for different time periods, many similarities were found
430 for the sources of particles at the site. The main source of smaller particles at the site in the
431 previous analysis is found to be the city centre in the northeast, for which relatively high
432 concentrations of NO_x were found. Similar is the case in the present analysis, as for the
433 sources found to be associated with north-easterly winds an association was also found with
434 NO_x and the LDSA_{ratio}. Additionally, a source of sulphate found with southerly winds was also
435 confirmed in the present study, with the association of high sulphate concentrations with a
436 factor, which presents higher contributions with winds from the southern sector. While in
437 the previous analysis the sources responsible for this source could not be pinpointed, in the
438 present analysis, using a back trajectory analysis, the sulphate factor was associated with
439 marine particle sources from all directions. Furthermore, a factor in the present analysis,
440 which identifies hot spots south of the measuring station with strong presence of PM of all
441 sizes, was also found with the k-means analysis in the previous study, though in that case it
442 was more associated with the pollution sources from that side rather than the long-range
443 transport found here.

444 These similarities are very encouraging, as even though the analyses were made for
445 different periods and using different methods, there is consistency between the results. This
446 means that regardless of the different seasons studied (previous analysis was performed
447 during winter to early spring), the sources of particles (and pollution) are relatively uniform,
448 without significant changes.

449 Additionally, the k-means method identified sets of conditions that either promote or
450 suppress the pollution at the sites (as this can be illustrated with the variable particle
451 concentrations between the clusters found from the analysis), rather than separate sources
452 of pollution that affect the site. While this provides a more realistic picture of the conditions
453 it makes it harder to distinguish the specific sources and their effect in its air quality. On the
454 other hand, the PMF not only provides clearer separation of the sources, but the temporal
455 contribution of each source as well, which shows the real extent of the effect of each source
456 of particles or pollutants, thus achieving source apportionment rather than just the
457 identification of pollution sources that the k-means offers. The k-means approach identifies
458 the effect of the sources of particles, but it also separates cleaner periods as separate
459 clusters. These two effects gives a more complete overall picture of the air quality at a site.
460 PMF could also provide this information, but it would be more difficult to obtain looking at
461 the different sources and the conditions that keep them to low contributions (this would
462 also require a much greater number of factors).

463 Furthermore, due to the complexity of the clusters from the k-means, pinpointing the
464 sources that the particles are associated with is difficult. This is due to the clusters, being a
465 set of different sources and conditions rather than clearly separated sources, were not
466 clearly associated with distinct wind directions, speeds or hot-spots. Contrary to that, the
467 factors formed by the PMF present clearer association with specific sectors, thus making it
468 easier to define the sources associated with them, as in the results they are presented as
469 hot spots within the polar plots.

470 The analysis of atmospheric data using either k-means or PMF are proven to provide
471 adequate and trustworthy information for the sources of particles and by extension of
472 pollution at a site, even with the sole use of LCS as shown in this paper and the preceding
473 Bousiotis et al. 2021 paper. The combined use of both approaches provides a clearer picture
474 of the different sources and their effect, as the PMF is able to better separate and provide
475 the effect of the sources of pollution that affect the air quality at a site and the k-means

476 provides a more realistic representation of the conditions at a site, by showing the
477 combined effect of these sources. The relative consistency of the results found between the
478 two analyses, even being in different time periods, is very encouraging and shows that the
479 very important information of pollution receptor modelling is viable with LCS, providing a
480 much-needed alternative for countries or scenarios where the use of regulatory-grade
481 instruments is not feasible. The significantly lower price point of LCSs means that in addition
482 to hyperlocal measurement of air pollution, it should now be possible to deliver hyperlocal
483 source apportionment of air pollution though as highlighted within this study, there are
484 some limitations for specific sources associated with pollutants with certain properties.
485 Further exploration of these limitations and design of methodologies to overcome them,
486 can enhance their capability and open new research and industrial abilities to pinpoint air
487 pollution sources and subsequently manage them.
488 Finally, the $LDSA_{ratio}$, a variable that was introduced in the previous analysis, was included in
489 the present one as well. As in the previous analysis, this ratio was found to be more
490 associated with fresher pollution from combustion sources near to the measuring station,
491 for which it has reliably performed in both analyses.

492

493 **5. Conclusions**

494 To solve air quality problems and to deliver the associated policy making effectively, it is
495 vital to have a methodology to measure the sources of air pollution, and their relative
496 importance. Historically, this has been achieved using expensive RG instruments. The cost
497 implications of these studies make assessment at dense spatial resolutions limited. In this
498 study, data from a low-cost OPC and other LCS, measuring gas phase pollutants, black
499 carbon and the lung deposited surface area of particles in BAQS were analysed using the
500 two-step PMF analysis. Four factors were formed from this analysis and were associated
501 with their respective sources and to a great extent with unique PNSD profiles. The following
502 factors were found: a factor associated with either combustion sources in close proximity of
503 the measurement site or associated with calm conditions, a marine factor, a factor
504 associated with midday activities from the city centre and a more constant factor from the
505 northeast. The same analysis was also performed using data from RG instruments and the
506 same PNSD factors. This was done to evaluate the results from the low-cost sensor analysis,

507 as well as to further characterise and clarify the sources associated with the factors formed.
508 Significant agreement was found between the results of the two analyses, highlighting that
509 the LCS are capable for carrying out such analyses. The additional ACSM data from the
510 second analysis further helped in the characterisation of the composition of the particles of
511 each factor, clarifying the sources associated with nitrate, sulphate and organic compounds
512 at the site, as well as strongly associating some with unique PNSD profiles. While in their
513 present state, the LCSs do not possess the full capability of the RG instruments for providing
514 high accuracy measurements, considering the limitations they were found to be adequate in
515 providing with the trends of the particles and pollutants measured which are important for
516 source apportionment studies. This is done at a fraction of the equipment cost; see
517 Bousiotis et al. 2021 for cost estimates.

518 Furthermore, comparing the results from the PMF to those from the k-means analysis
519 showed the different strengths and weaknesses of each approach. The PMF is better in
520 pinpointing the effect of separate sources of pollution, but it is difficult to give a clear
521 representation of the actual conditions when each factor affects the site. The k-means is not
522 as efficient in clearly separating the different sources, but it does provide a more realistic
523 picture of the air quality at a site in relation to the ambient conditions. The combined use of
524 both methods though provided a clearer picture for the conditions at the site.

525 The methodologies developed and used in this study will help to reliably facilitate source
526 apportionment studies in the future, with either the sole use of LCS or their combination
527 with RG instruments. As for a given site, specific PNSD formations are associated with
528 specific conditions and sources (Harrison et al., 2011), by creating a repository of unique
529 PNSDs at a site and associating them with their respective sources, in the future the source
530 apportionment may be done to an extend using only PNSD profiles and meteorological data
531 alone. This will do much in simplifying the source apportionment process allowing its wider
532 application and help in dealing with environmental challenges, though it can be challenging
533 in sites with particle emissions smaller than what the OPC can measure (ex. vehicle exhaust
534 emissions). For this though, further testing in more diverse environments and scenarios is
535 needed which, along with the anticipated development of the LCS, will provide a denser and
536 reliable measuring network even for countries with lower incomes and help for cleaner and
537 healthier environmental conditions.

538

539

540 **Author Contributions**

541 The study was conceived and planned by FDP who also contributed to the final manuscript,
542 and DB who carried out the analysis and prepared the first draft. AS, MH, DCSB and SD
543 provided data for the analysis. DCSB provided help with the analysis of the data. RMH, PME
544 and AB contributed to the final manuscript.

545

546 **Competing Interests**

547 The authors have no conflict of interests.

548

549 **Acknowledgements**

550 We thank the OSCA team (Integrated Research Observation System for Clean Air) at the
551 Birmingham Air Quality Supersite (BAQS), funded by NERC (NE/T001909/1), for help in data
552 collection for the regulatory-grade instruments. We thank Lee Chapman for access to his
553 meteorological dataset used in the analysis.

554 **Financial support.**

555 This research has been supported by the Natural Environment Research Council (NERC grant
556 no. NE/T001879/1), the Engineering and Physical Sciences Research Council (EPSRC grant
557 no. EP/T030100/1) and internal EPSRC funding provided to the University of Birmingham for
558 Impact Acceleration.

559

560

561 **References**

562

563 Austin, E., Novosselov, I., Seto, E. and Yost, M. G.: Laboratory evaluation of the Shinyei
564 PPD42NS low-cost particulate matter sensor, *PLoS One*, 10(9), 1–17,
565 doi:10.1371/journal.pone.0137789, 2015.

566

567 Beddows, D. C. S., Harrison, R. M., Green, D. C. and Fuller, G. W.: Receptor modelling of both
568 particle composition and size distribution from a background site in London, UK, *Atmos.*
569 *Chem. Phys.*, 15(17), 10107–10125, doi:10.5194/acp-15-10107-2015, 2015.

570

571 Beddows, D.C.S., and Harrison, R.M.: Receptor modelling of both particle composition and
572 size distribution from a background site in London, UK – a two-step approach, *Atmos. Chem.*
573 *Phys.*, 19, 39 – 55, <https://doi.org/10.5194/acp-19-39-2019>, 2019.

574

575 Bousiotis, D., Pope, F.D., Beddows, D.C.S., Dall'Osto, M., Massling, A., Nøjgaard, J.K.,
576 Nordstrøm, C., Niemi, J.V., Portin, H., Petäjä, T., Perez, N., Alastuey, A., Querol, X.,
577 Kouvarakis, G., Mihalopoulos, N., Vratolis, S., Eleftheriadis, K., Wiedensohler A., Weinhold,
578 A., Merkel, M., Tuch, T. and Harrison R.M.: A phenomenology of new particle formation
579 (NPF) at 13 European sites, *Atmos. Chem. Phys.*, 21, 11905 - 11925,
580 <https://doi.org/10.5194/acp-21-11905-2021>, 2021.

581 Bousiotis, D., Singh, A., Haugen, M., Beddows, D.C.S., Diez, S., Edwards, P.M., Boies, A.,
582 Harrison, R.M. and Pope, F.D.: Assessing the sources of particles at an urban background site
583 using both regulatory grade instruments and low-cost sensors – A comparative study,
584 *Atmos. Meas. Tech.*, 14, 4139 – 4155, <https://doi.org/10.5194/amt-14-4139-2021>, 2021.

585

586 Carslaw, D. C. and Ropkins, K.: openair — An R package for air quality data analysis, *Environ.*
587 *Model. Softw.*, 27–28, 52–61, doi:10.1016/j.envsoft.2011.09.008, 2012.

588

589 Crilley, L. R., Shaw, M., Pound, R., Kramer, L. J., Price, R., Young, S., Lewis, A. C., and Pope, F.
590 D.: Evaluation of a low-cost optical particle counter (Alphasense OPC-N2) for ambient air

591 monitoring, *Atmos. Meas. Tech.*, 11, 709–720, <https://doi.org/10.5194/amt-11-709-2018>,
592 2018.

593

594 Crilley, L. R., Singh, A., Kramer, L. J., Shaw, M. D., Alam, M. S., Apte, J. S., Bloss, W. J.,
595 Hildebrandt Ruiz, L., Fu, P., Fu, W., Gani, S., Gatari, M., Ilyinskaya, E., Lewis, A. C., Ng'ang'a,
596 D., Sun, Y., Whitty, R. C. W., Yue, S., Young, S. and Pope, F. D.: Effect of aerosol composition
597 on the performance of low-cost optical particle counter correction factors, *Atmos. Meas.*
598 *Tech.*, 13(3), 1181–1193, doi:10.5194/amt-13-1181-2020, 2020.

599

600 Draxler, R. R. and Hess, G. D.: An Overview of the HYSPLIT_4 Modelling System for
601 Trajectories, Dispersion, and Deposition, *Aust. Meteorol. Mag.*, 47(January), 295–308, 1998.

602

603 De Vito, S., Esposito, E., Castell, N., Schneider, P. and Bartonova, A.: On the robustness of
604 field calibration for smart air quality monitors, *Sensors Actuators, B Chem.*, 310(July 2019),
605 127869, doi:10.1016/j.snb.2020.127869, 2020.

606

607 Feinberg, S. N., Williams, R., Hagler, G., Low, J., Smith, L., Brown, R., Garver, D., Davis, M.,
608 Morton, M., Schaefer, J. and Campbell, J.: Examining spatiotemporal variability of urban
609 particulate matter and application of high-time resolution data from a network of low-cost
610 air pollution sensors, *Atmos. Environ.*, 213(May), 579–584,
611 doi:10.1016/j.atmosenv.2019.06.026, 2019.

612 Giordano, M.R, Malings, C., Pandis, S.N., Presto, A.A., McNeill, V.F., Westervelt, D.M.,
613 Beekmann, M., and Subramanian, R.: From low-cost sensors to high-quality data: A
614 summary of challenges and best practices for effectively calibrating low-cost particulate
615 matter mass sensors, *Journal of Aerosol Science*,
616 <https://doi.org/10.1016/j.jaerosci.2021.105833>, 2021.

617 Hagan, D. H., Gani, S., Bhandari, S., Patel, K., Habib, G., Apte, J. S., Hildebrandt Ruiz, L. and
618 Kroll, J. H.: Inferring Aerosol Sources from Low-Cost Air Quality Sensor Measurements: A
619 Case Study in Delhi, India, *Environ. Sci. Technol. Lett.*, 6(8), 467–472,
620 doi:10.1021/acs.estlett.9b00393, 2019.

621
622 Hagan, D. and Kroll, J.: Assessing the accuracy of low-cost optical particle sensors using a
623 physics-based approach, *Atmos. Meas. Tech.*, 6343–6355, doi:10.5194/amt-13-6343-2020,
624 2020.
625
626 Harrison, R. M., Beddows, D. C. S. and Dall'Osto, M.: PMF analysis of wide-range particle size
627 spectra collected on a major highway, *Environ. Sci. Technol.*, 45(13), 5522–5528,
628 doi:10.1021/es2006622, 2011.
629
630 Haugen, M.J., Singh, A., Bousiotis, D., Pope, F.D., Boies, A.M.: Demonstrating the ability to
631 differentiate between semi-volatile and solid particle events with low-cost lung-deposited
632 surface area and black carbon particle sensors, *Atmosphere*, 13, 747,
633 doi:10.3390/atmos13050747, 2022.
634
635 Hopke, P. K.: Review of receptor modeling methods for source apportionment, *J. Air Waste*
636 *Manag. Assoc.*, 66(3), 237–259, doi:10.1080/10962247.2016.1140693, 2016.
637
638 Jovašević-Stojanović, M., Bartonova, A., Topalović, D., Lazović, I., Pokrić, B. and Ristovski, Z.:
639 On the use of small and cheaper sensors and devices for indicative citizen-based monitoring
640 of respirable particulate matter, *Environ. Pollut.*, 206, 696–704,
641 doi:10.1016/j.envpol.2015.08.035, 2015.
642
643 Kan, H., Chen, B. and Hong, C.: Health impact of outdoor air pollution in China: Current
644 knowledge and future research needs, *Environ. Health Perspect.*, 117(5), 12737,
645 doi:10.1289/ehp.12737, 2009.
646
647 Kanaroglou, P. S., Jerrett, M., Morrison, J., Beckerman, B., Arain, M. A., Gilbert, N. L. and
648 Brook, J. R.: Establishing an air pollution monitoring network for intra-urban population
649 exposure assessment: A location-allocation approach, *Atmos. Environ.*, 39(13), 2399–2409,
650 doi:10.1016/j.atmosenv.2004.06.049, 2005.

651

652 Kosmopoulos, G., Salamalikis, V., Pandis, S. N., Yannopoulos, P., Bloutsos, A. A. and
653 Kazantzidis, A.: Low-cost sensors for measuring airborne particulate matter: Field evaluation
654 and calibration at a South-Eastern European site, *Sci. Total Environ.*, 748(October), 141396,
655 doi:10.1016/j.scitotenv.2020.141396, 2020.

656

657 Krause, A., Zhao, J. and Birmili, W.: Low-cost sensors and indoor air quality: A test study in
658 three residential homes in Berlin, Germany, *Gefahrstoffe Reinhaltung der Luft*, 79(3), 87–94,
659 doi:10.37544/0949-8036-2019-03-49, 2019.

660

661 Leoni, C., Pokorná, P., Hovorka, J., Masiol, M., Topinka, J., Zhao, Y., Křůmal, K., Cliff, S.,
662 Mikuška, P. and Hopke, P. K.: Source apportionment of aerosol particles at a European air
663 pollution hot spot using particle number size distributions and chemical composition,
664 *Environ. Pollut.*, 234, 145–154, doi:10.1016/j.envpol.2017.10.097, 2018.

665

666 Lepistö, T., Kuuluvainen, H., Lintusaari, H., Kuittinen, N., Salo, L., Helin, A., Niemi, J.V.,
667 Manninen, H.E., Timonen, H., Jalava, P., Saarikoski, S. and Rönkkö, T.: Connection between
668 lung deposited surface area (LDSA) and black carbon (BC) concentrations in road traffic and
669 harbour environments, *Atmospheric Environment*, 272, 118931,
670 <https://doi.org/10.1016/j.atmosenv.2021.118931>, 2022.

671

672 Lewis, A. C., von Schneidmesser, E. and Peltier, R. E.: Low-cost sensors for the
673 measurement of atmospheric composition: overview of topic and future applications.
674 WMO-No. 1215, World Meteorological Organization, Geneva, Switzerland, 46pp., 2018.

675

676 Liang, Y., Wu, C., Jiang, S., Li, Y. J., Wu, D., Li, M., Cheng, P., Yang, W., Cheng, C., Li, L., Deng,
677 T., Sun, J. Y., He, G., Liu, B., Yao, T., Wu, M. and Zhou, Z.: Field comparison of
678 electrochemical gas sensor data correction algorithms for ambient air measurements,
679 *Sensors Actuators, B Chem.*, 327(November 2020), doi:10.1016/j.snb.2020.128897, 2021.

680

681 Lin, C. T., Baker, A. R., Jickells, T. D., Kelly, S. and Lesworth, T.: An assessment of the
682 significance of sulphate sources over the Atlantic Ocean based on sulphur isotope data,

683 Atmos. Environ., 62, 615–621, doi:10.1016/j.atmosenv.2012.08.052, 2012.
684
685 Mahbub, P., Ayoko, G.A., Goonetilleke, A., Egodawatta, P.: Analysis of the build-up of semi
686 and non volatile organic compounds on urban roads, Water Res. 45(9), 2835 - 2844, doi:
687 10.1016/j.watres.2011.02.033, 2011.
688
689 Manisalidis, I., Stavropoulou, E., Stavropoulos, A. and Bezirtzoglou, E.: Environmental and
690 Health Impacts of Air Pollution: A Review, Front. Public Heal., 8(February), 1–13,
691 doi:10.3389/fpubh.2020.00014, 2020.
692
693 Mannucci, P. M. and Franchini, M.: Health effects of ambient air pollution in developing
694 countries, Int. J. Environ. Res. Public Health, 14(9), 1–8, doi:10.3390/ijerph14091048, 2017.
695
696 Miskell, G., Salmond, J. A. and Williams, D. E.: Use of a handheld low-cost sensor to explore
697 the effect of urban design features on local-scale spatial and temporal air quality variability,
698 Sci. Total Environ., 619–620, 480–490, doi:10.1016/j.scitotenv.2017.11.024, 2018.
699
700 Moore, F. C.: Climate change and air pollution: Exploring the synergies and potential for
701 mitigation in industrializing countries, Sustainability, 1(1), 43–54, doi:10.3390/su1010043,
702 2009.
703
704 Nagendra, S., Reddy Yasa, P., Narayana, M., Khadirnaikar, S. and Pooja Rani: Mobile
705 monitoring of air pollution using low cost sensors to visualize spatio-temporal variation of
706 pollutants at urban hotspots, Sustain. Cities Soc., 44(September 2018), 520–535,
707 doi:10.1016/j.scs.2018.10.006, 2019.
708
709 Omokungbe, O. R., Fawole, O. G., Owoade, O. K., Popoola, O. A. M., Jones, R. L., Olise, F. S.,
710 Ayoola, M. A., Abiodun, P. O., Teyeje, A. B., Olufemi, A. P., Sunmonu, L. A. and Abiye, O. E.:
711 Analysis of the variability of airborne particulate matter with prevailing meteorological
712 conditions across a semi-urban environment using a network of low-cost air quality sensors,
713 Heliyon, 6(6), e04207, doi:10.1016/j.heliyon.2020.e04207, 2020.
714

715 Paatero, P. and Tapper, U.: Analysis of different modes of factor analysis as least squares fit
716 problems, *Chemom. Intell. Lab. Syst.*, 18(2), 183–194, doi:10.1016/0169-7439(93)80055-M,
717 1993.

718

719 Paatero, P. and Tapper, U.: Positive Matrix Factorization : A Non-negative factor model with
720 optimal utilization of error estimates of data values, *Environmetrics*, 5(April 1993), 111–126,
721 1994.

722

723 Paatero, P., Hopke, P. K., Song, X.-H., and Ramadan, Z.: Understanding and controlling
724 rotations in factor analytic models, *Chemometr. Intell. Lab.*, 60, 253–264, 2002.

725

726 Paatero P.: User’s guide for positive matrix factorization programs PMF2 and PMF3, Part1:
727 tutorial. University of Helsinki, Helsinki, Finland, 2004a.

728

729 Paatero P.: User’s guide for positive matrix factorization programs PMF2 and PMF3, Part2:
730 references. University of Helsinki, Helsinki, Finland, 2004b.

731

732 Pascal, M., Corso, M., Chanel, O., Declercq, C., Badaloni, C., Cesaroni, G., Henschel, S.,
733 Meister, K., Haluza, D., Martin-Olmedo, P. and Medina, S.: Assessing the public health
734 impacts of urban air pollution in 25 European cities: Results of the Aphekom project, *Sci.*
735 *Total Environ.*, 449(2007105), 390–400, doi:10.1016/j.scitotenv.2013.01.077, 2013.

736

737 Penza, M.: *Low-cost sensors for outdoor air quality monitoring*, Elsevier Inc., 2019.

738 Petkova, E. P., Jack, D. W., Volavka-Close, N. H. and Kinney, P. L.: Particulate matter
739 pollution in African cities, *Air Qual. Atmos. Heal.*, 6(3), 603–614, doi:10.1007/s11869-013-
740 0199-6, 2013.

741

742 Pokorná, P., Hovorka, J. and Hopke, P. K.: Elemental composition and source identification
743 of very fine aerosol particles in a European air pollution hot-spot, *Atmos. Pollut. Res.*, 7(4),
744 671–679, doi:10.1016/j.apr.2016.03.001, 2016.

745

746 Pope, F. D., Gatari, M., Ng’ang’a, D., Poynter, A. and Blake, R.: Airborne particulate matter

747 monitoring in Kenya using calibrated low cost sensors, *Atmos. Chem. Phys.*, 15403–15418,
748 doi:10.5194/acp-18-15403-2018, 2018.

749

750 Popoola, O. A. M., Carruthers, D., Lad, C., Bright, V. B., Mead, M. I., Stettler, M. E. J., Saffell,
751 J. R. and Jones, R. L.: Use of networks of low cost air quality sensors to quantify air quality in
752 urban settings, *Atmos. Environ.*, 194(February), 58–70,
753 doi:10.1016/j.atmosenv.2018.09.030, 2018.

754

755 Prakash, J., Choudhary, S., Raliya, R., Chadha, T., Fang, J., George, M. P. and Biswas, P.:
756 Deployment of Networked Low-Cost Sensors and Comparison to Real-Time Stationary
757 Monitors in New Delhi, *J. Air Waste Manage. Assoc.*, 71:11, 1347-1360,
758 doi:10.1080/10962247.2021.1890276, 2021.

759

760 Raes, F., Dingenen, R. Van, Elisabetta, V., Wilson, J., Putaud, J. P., Seinfeld, J. H. and Adams,
761 P.: Formation and cycling of aerosols in the global troposphere, *Atmos. Environ.*, 34, 4215–
762 4240, 2000.

763

764 Reff, A., Eberly, S. I. and Bhave, P. V.: Receptor Modeling of Ambient Particulate Matter Data
765 Using Positive Matrix Factorization: Review of Existing Methods, *J. Air Waste Manage.*
766 *Assoc.*, 57(2), 146–154, doi:10.1080/10473289.2007.10465319, 2007.

767

768 Rivas, I., Vicens, L., Basagaña, X., Tobías, A., Katsouyanni, K., Walton, H., Hüglin, C., Alastuey,
769 A., Kulmala, M., Harrison, R. M., Pekkanen, J., Querol, X., Sunyer, J. and Kelly, F. J.:
770 Associations between sources of particle number and mortality in four European cities,
771 *Environ. Int.*, 155(May), doi:10.1016/j.envint.2021.106662, 2021.

772

773 Schneider, P., Castell, N., Vogt, M., Dauge, F. R., Lahoz, W. A. and Bartonova, A.: Mapping
774 urban air quality in near real-time using observations from low-cost sensors and model
775 information, *Environ. Int.*, 106(May), 234–247, doi:10.1016/j.envint.2017.05.005, 2017.

776

777 Schnelle-Kreis, J., Sklorz, M., Orasche, J., Stölzel, M., Peters, A. and Zimmermann, R.: Semi
778 volatile organic compounds in ambient PM_{2.5}. Seasonal trends and daily resolved source

779 contributions, *Environ. Sci. Technol.*, 41(11), 3821–3828, doi:10.1021/es060666e, 2007.
780

781 Shafran-Nathan, R., Etzion, Y., Zivan, O. and Broday, D. M.: Estimating the spatial variability
782 of fine particles at the neighborhood scale using a distributed network of particle sensors,
783 *Atmos. Environ.*, 218(April), 117011, doi:10.1016/j.atmosenv.2019.117011, 2019.
784

785 Shindler, L.: Development of a low-cost sensing platform for air quality monitoring:
786 application in the city of Rome, *Environ. Technol. (United Kingdom)*, 42(4), 618–631,
787 doi:10.1080/09593330.2019.1640290, 2021.
788

789 Shiraiwa, M., Ueda, K., Pozzer, A., Lammel, G., Kampf, C. J., Fushimi, A., Enami, S., Arangio,
790 A. M., Fröhlich-Nowoisky, J., Fujitani, Y., Furuyama, A., Lakey, P. S. J., Lelieveld, J., Lucas, K.,
791 Morino, Y., Pöschl, U., Takahama, S., Takami, A., Tong, H., Weber, B., Yoshino, A. and Sato,
792 K.: Aerosol Health Effects from Molecular to Global Scales, *Environ. Sci. Technol.*, 51(23),
793 13545–13567, doi:10.1021/acs.est.7b04417, 2017.
794

795 Smith, K. R., Edwards, P. M., Ivatt, P. D., Lee, J. D., Squires, F., Dai, C., Peltier, R. E., Evans, M.
796 J., Sun, Y., and Lewis, A. C.: An improved low-power measurement of ambient NO₂ and O₃
797 combining electrochemical sensor clusters and machine learning, *Atmos. Meas. Tech.*, 12,
798 1325–1336, doi:10.5194/amt-12-1325-2019, 2019.
799

800 Sousan, S., Koehler, K., Thomas, G., Park, J. H., Hillman, M., Halterman, A. and Peters, T. M.:
801 Inter-comparison of low cost sensors for measuring the mass concentration of occupational
802 aerosols, *Aerosol Sci. Technol.*, 50(5), 462–473, doi:10.1080/02786826.2016.1162901, 2016.
803

804 Utsunomiya, A. and Wakamatsu, S.: Temperature and humidity dependence on aerosol
805 composition in the northern Kyushu, Japan, *Atmos. Environ.*, 30(13), 2379–2386,
806 doi:10.1016/1352-2310(95)00350-9, 1996.
807

808 Vajs, I., Drajić, D., Gligorić, N., Radovanović, I. and Popović, I.: Developing relative humidity
809 and temperature corrections for low-cost sensors using machine learning, *Sensors*, 21(10),
810 doi:10.3390/s21103338, 2021.

811

812 Valavanidis, A., Fiotakis, K. and Vlachogianni, T.: Airborne particulate matter and human
813 health: Toxicological assessment and importance of size and composition of particles for
814 oxidative damage and carcinogenic mechanisms, *J. Environ. Sci. Heal. - Part C Environ.*
815 *Carcinog. Ecotoxicol. Rev.*, 26(4), 339–362, doi:10.1080/10590500802494538, 2008.

816

817 Wang, P., Xu, F., Gui, H., Wang, H. and Chen, D. R.: Effect of relative humidity on the
818 performance of five cost-effective PM sensors, *Aerosol Sci. Technol.*, 55(8), 957–974,
819 doi:10.1080/02786826.2021.1910136, 2021.

820

821 Weissert, L., Alberti, K., Miles, E., Miskell, G., Feenstra, B., Henshaw, G. S., Papapostolou, V.,
822 Patel, H., Polidori, A., Salmond, J. A. and Williams, D. E.: Low-cost sensor networks and land-
823 use regression: Interpolating nitrogen dioxide concentration at high temporal and spatial
824 resolution in Southern California, *Atmos. Environ.*, 223(January), 117287,
825 doi:10.1016/j.atmosenv.2020.117287, 2020.

826

827 Whitty, R. C. W., Pfeffer, M. A., Ilyinskaya, E., Roberts, T. J., Schmidt, A., Barsotti, S., Strauch,
828 W., Crilley, L. R., Pope, F. D., Bellanger, H., Mendoza, E., Mather, T. A., Liu, E., Peters,
829 N., Taylor, I. A., Francis, H., Hernandez Leiva, X., Lynch, D., Nobert, S., Baxter, P.:
830 Effectiveness of low-cost air quality monitors for identifying volcanic SO₂ and PM downwind
831 from Masaya volcano, Nicaragua. *Volcanica*, 5 (1),doi:
832 <https://doi.org/10.30909/vol.05.01.3359>, 2022.

833

834 WHO global air quality guidelines. Particulate matter (PM_{2.5} and PM₁₀), ozone, nitrogen
835 dioxide, sulfur dioxide and carbon monoxide, World Health Organisation, ISBN 978-92-4-
836 003443-3, Licence: CC BY-NC-SA 3.0 IGO, Geneva, 2021

837

838 Wu, S., Ni, Y., Li, H., Pan, L., Yang, D., Baccarelli, A. A., Deng, F., Chen, Y., Shima, M. and Guo,
839 X.: Short-term exposure to high ambient air pollution increases airway inflammation and
840 respiratory symptoms in chronic obstructive pulmonary disease patients in Beijing, China,
841 *Environ. Int.*, 94, 76–82, doi:10.1016/j.envint.2016.05.004, 2016.

842

843 Xu, Y., Zhang, J.S.: Understanding SVOCs, ASHRAE Journal, 53 (12), 121 - 125, 2011.

844

845 Zeger, S. L., Dominici, F., McDermott, A. and Samet, J. M.: Mortality in the medicare
846 population and Chronic exposure to fine Particulate air pollution in urban centers (2000-
847 2005), Environ. Health Perspect., 116(12), 1614–1619, doi:10.1289/ehp.11449, 2008.

848

849 **FIGURE LEGENDS**

850

851 **Figure 1:** Map of the measuring station.

852

853 **Figure 2:** Particle profiles of the factors from the PMF analysis (> 500 nm). The lines
854 indicate the average particle count per second for each particle size bin.

855

856 **Figure 3:** Variable association for the factors from the LC analysis. Grey bars indicate
857 the values of F, while red bars indicate the explained variations for each
858 variable.

859

860 **Figure 4:** Temporal variation of the contributions of the factors from the LC analysis. The
861 windroses refer to the wind conditions for the corresponding periods when
862 specific factors presented higher G contributions.

863

864 **Figure 5:** Polar plot of the average G contributions of the factors from the LC analysis.

865

866 **Figure 6:** Average G contribution of the factors from the LC analysis for incoming air
867 masses. Higher contributions indicate better association of the given factor
868 with the corresponding air mass origin.

869

870 **Figure 7:** Variable association for the factors from the RG analysis. Grey bars indicate the
871 values of F, while red bars indicate the explained variations for each variable.

872

873 **Figure 8:** Polar plot of the average G contributions of the factors from the RG analysis.

874

875 **Figure 9:** Average G contribution of the factors from the RG analysis for incoming air
876 masses. Higher contributions indicate better association of the given factor
877 with the corresponding air mass origin.

878

879



880

881

Figure 1: Map of the measuring station. Imagery ©2022 Bluesky, Getmapping plc, Infoterra

882

Ltd & Bluesky, Maxar Technologies, The GeoInformation Group, Map data

883

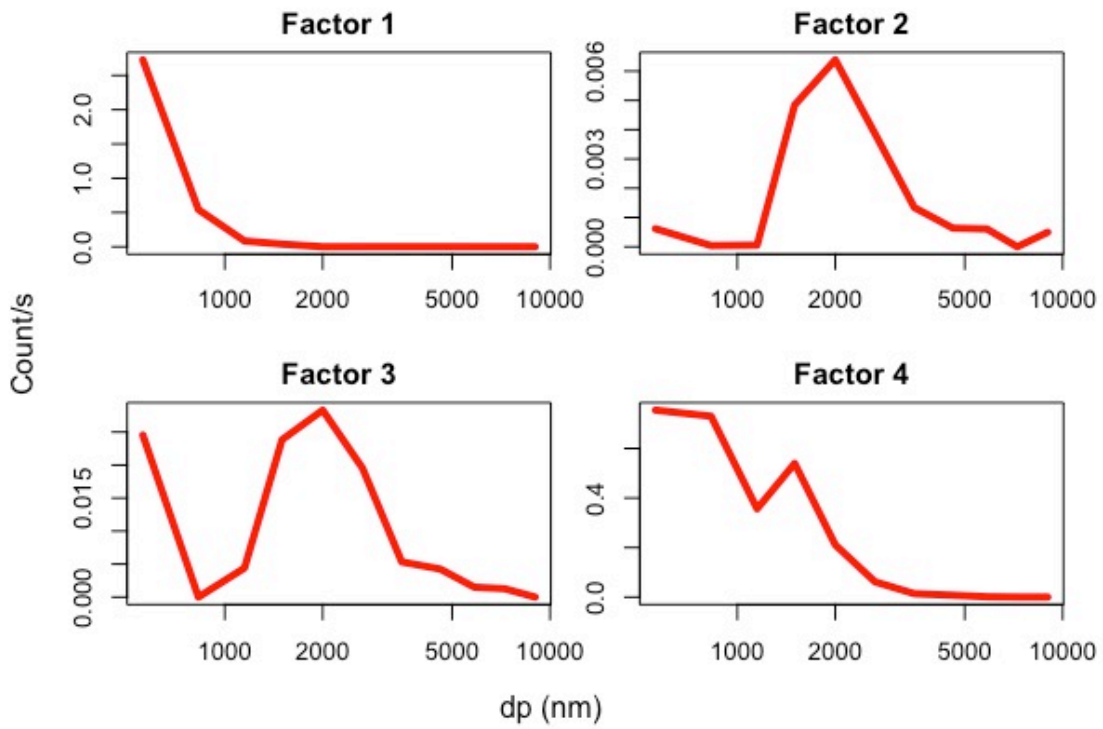
©2022

884

885

886

887

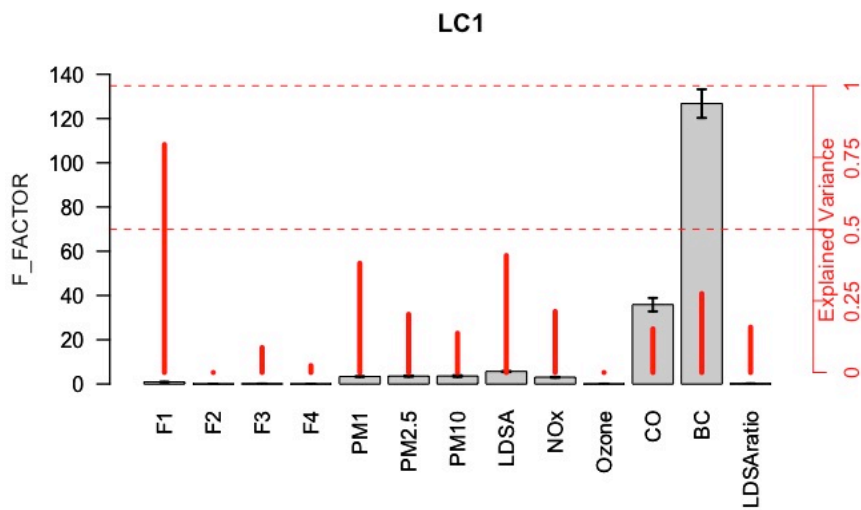


888

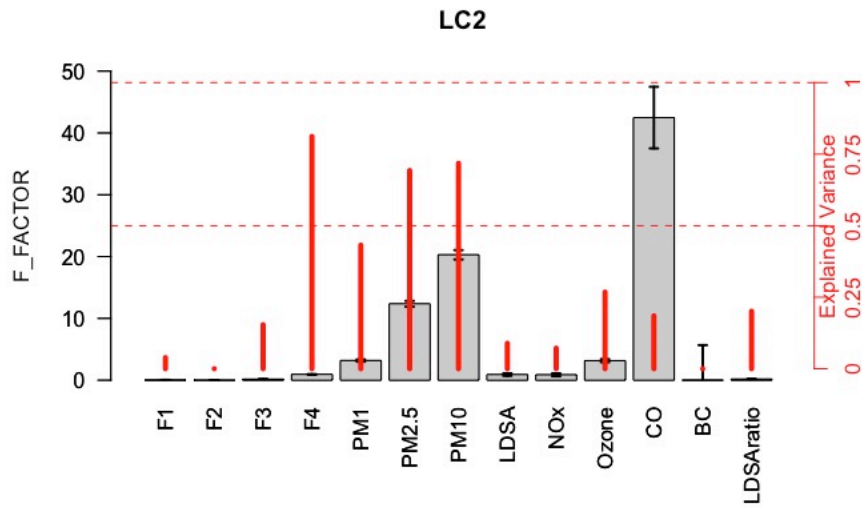
889 Figure 2: Particle profiles of the factors from the PMF analysis (above 500 nm). The lines

890 indicate the average particle count per second for each particle size bin.

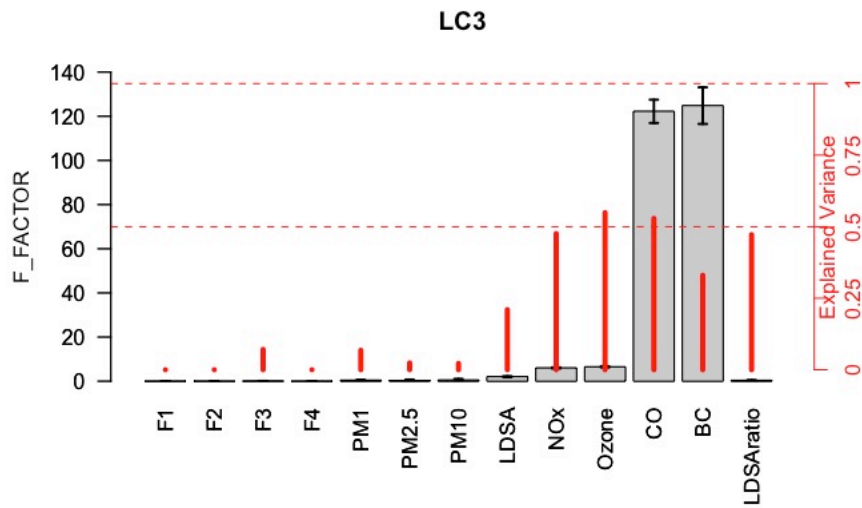
891



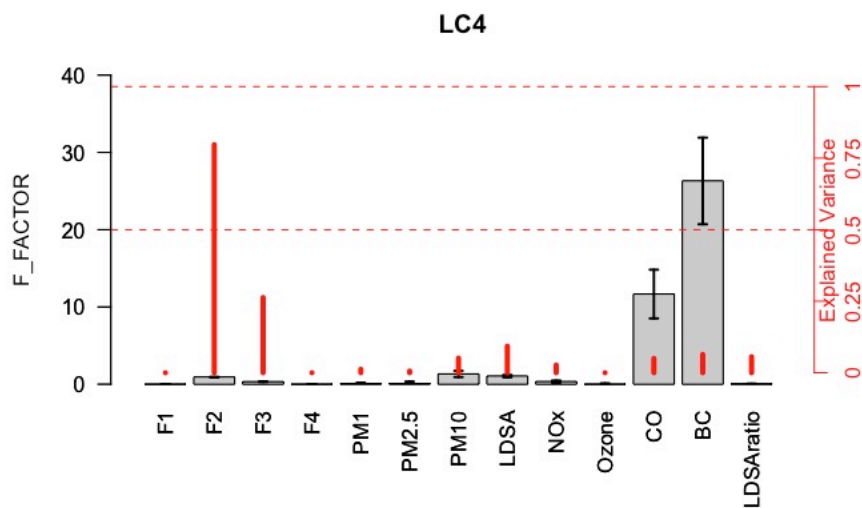
892



893



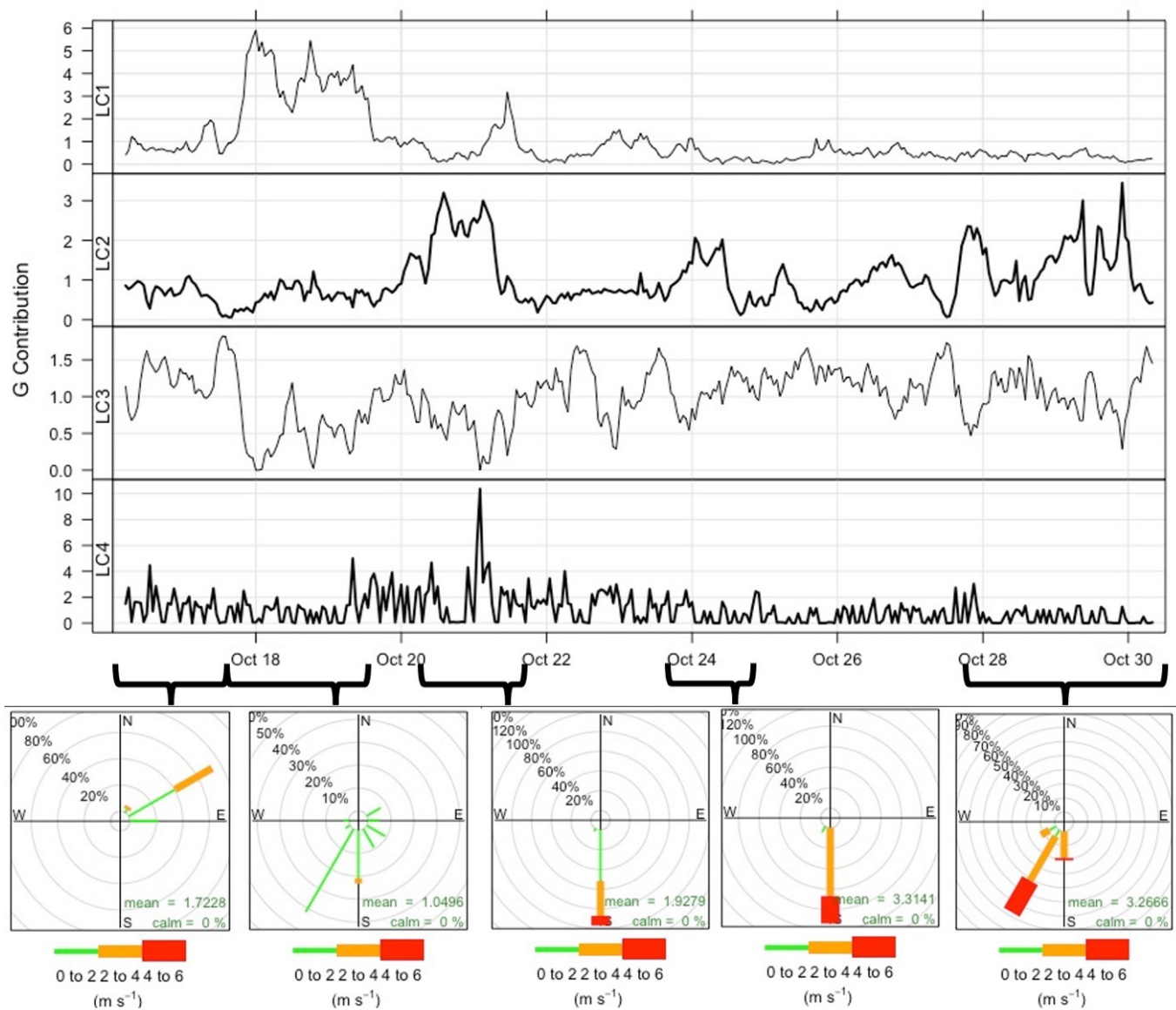
894



895

896 Figure 3: Contribution of the factors from the LC analysis. Grey bars indicate the values of F,
 897 while red bars indicate the explained variations for each variable.

898

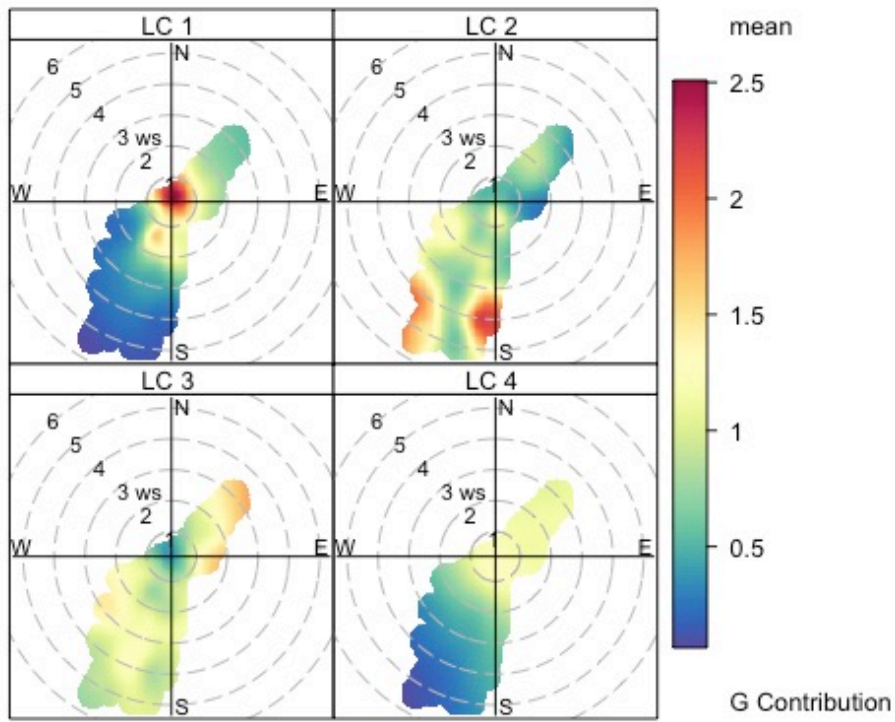


899

Frequency of counts by wind direction (%)

900 Figure 4: Temporal variation of the contributions of the factors from the LC analysis. The
 901 windroses refer to the wind conditions for the corresponding periods when specific factors
 902 presented higher G contributions.

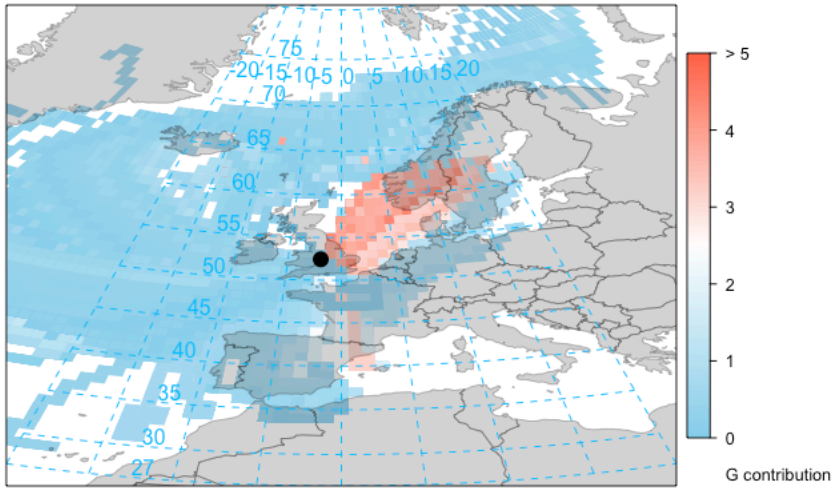
903



904

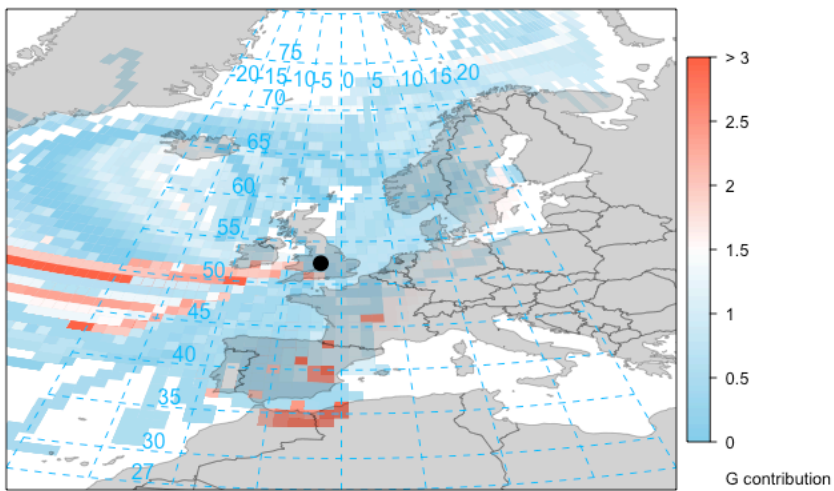
905 Figure 5: Polar plot of the average G contributions of the factors from the LC analysis.

906



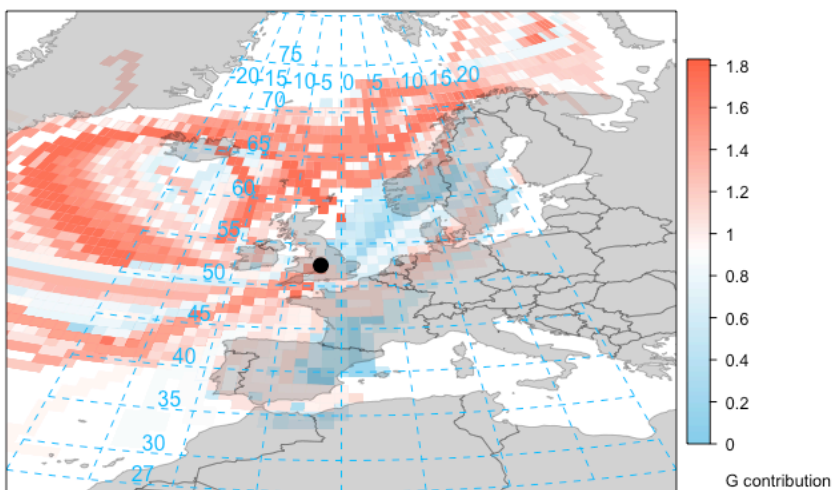
907

LC1



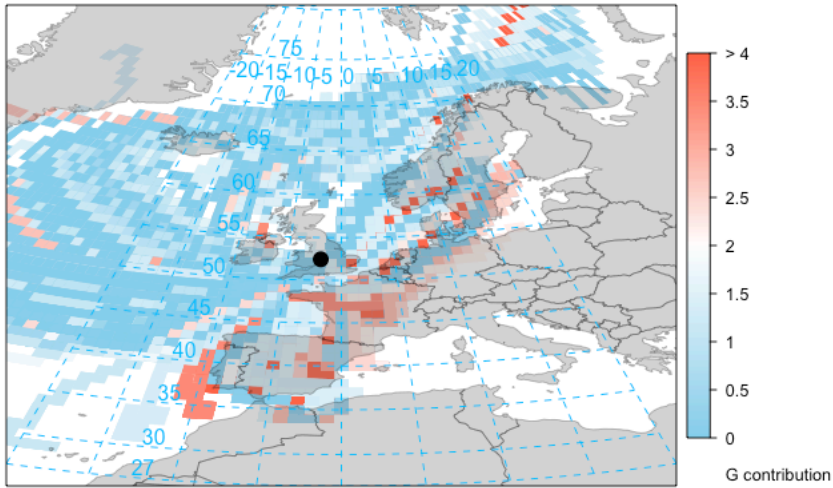
908

LC2



909

LC3



910

LC4

911 Figure 6: Average G contribution of the factors from the LC analysis for incoming air masses.

912 Higher contributions indicate better association of the given factor with the corresponding

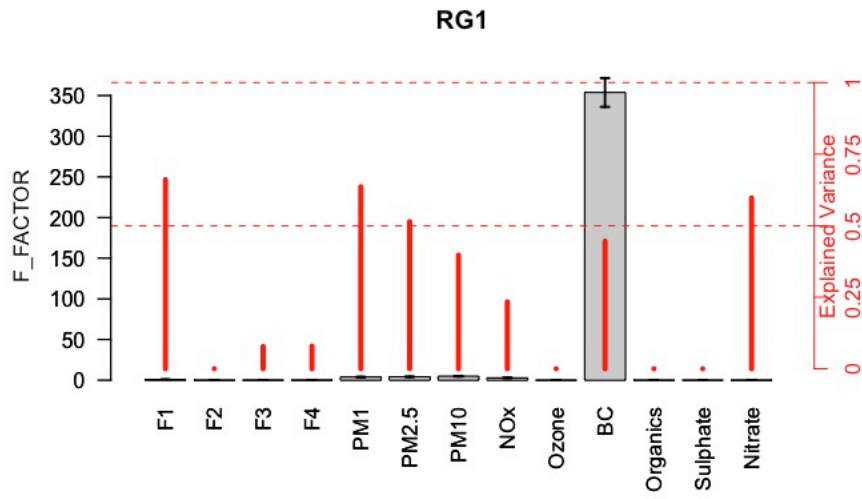
913 air mass origin.

914

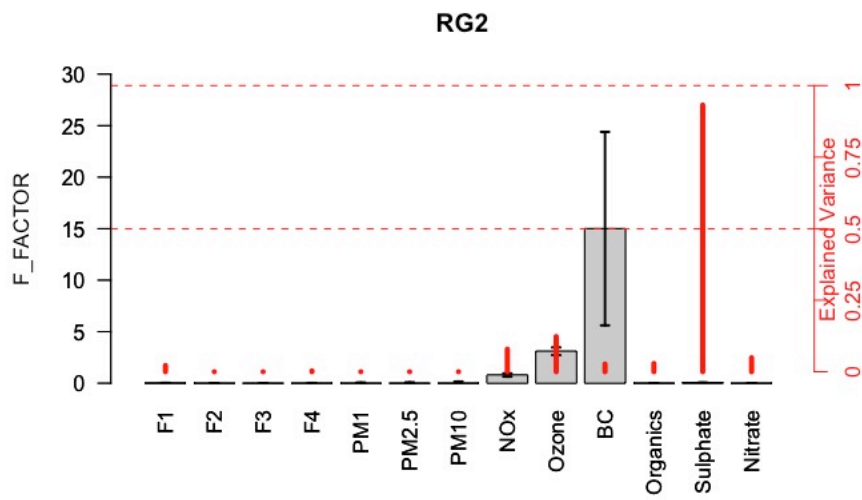
915

916

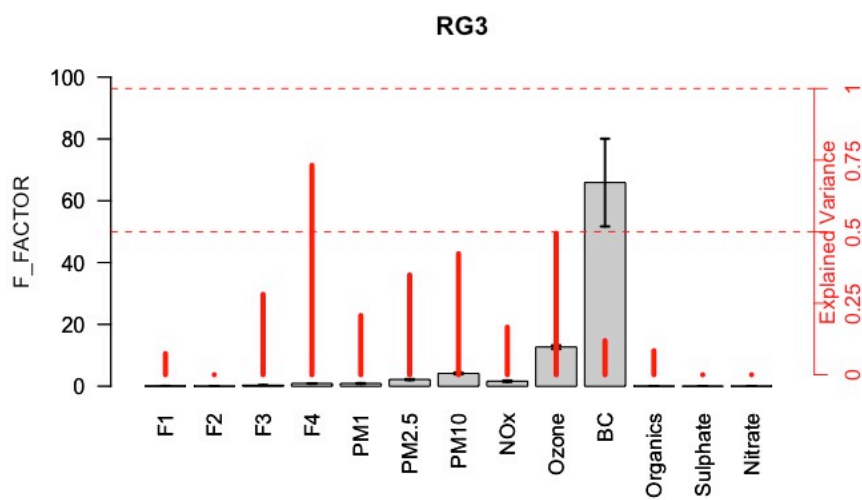
917
918

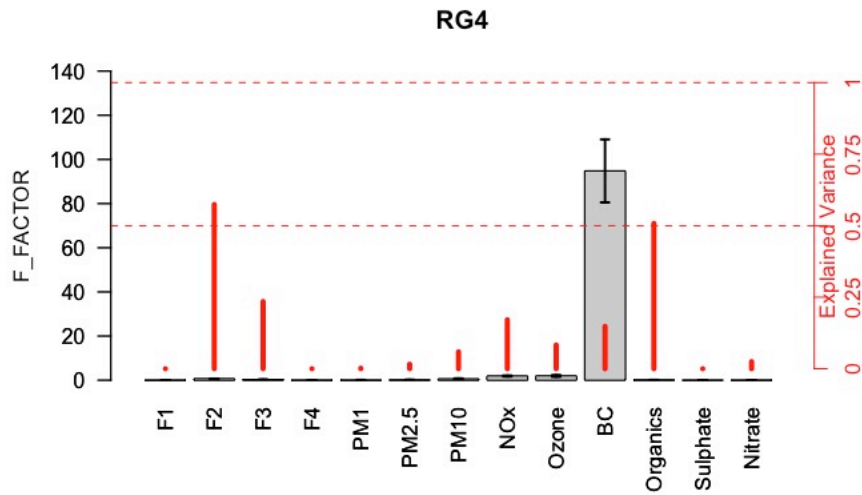


919



920



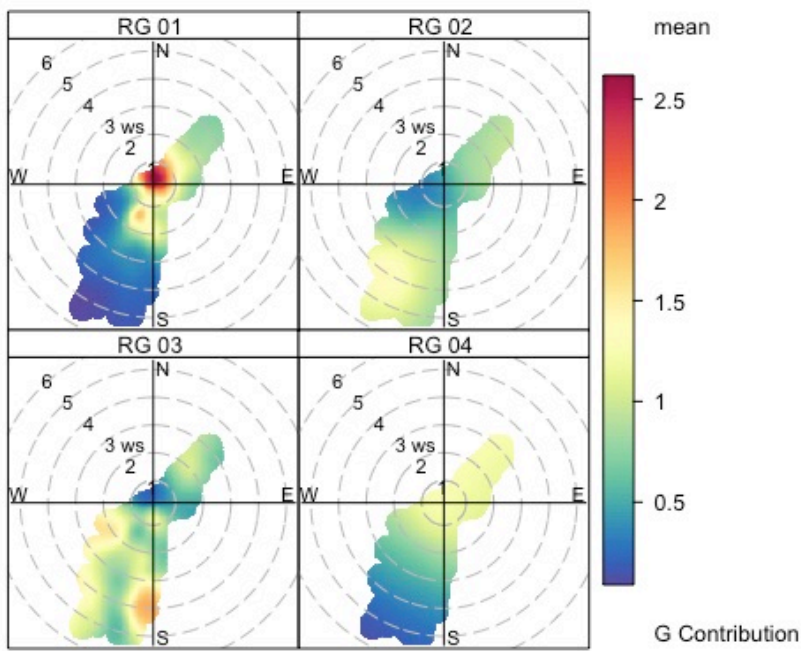


921

922 Figure 7: Variable association for the factors from the RG analysis. Grey bars indicate the
 923 values of F, while red bars indicate the explained variations for each variable.

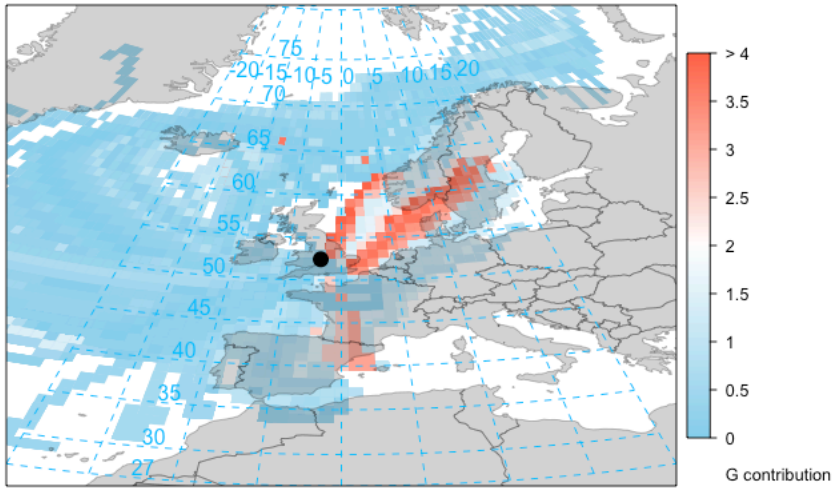
924

925



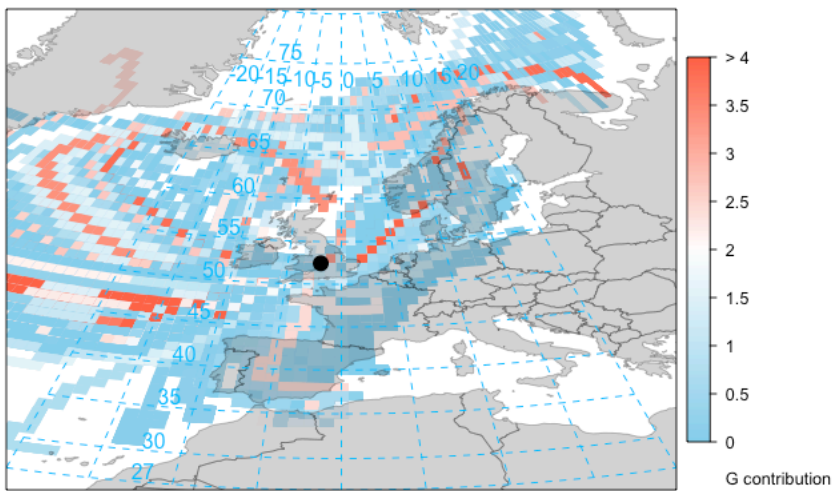
926

927 Figure 8: Polar plot of the average G contributions of the factors from the RG analysis.



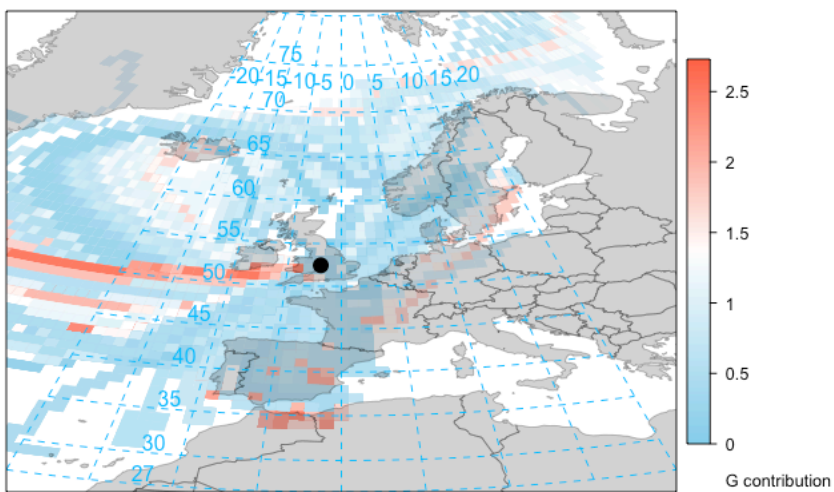
928

RG1



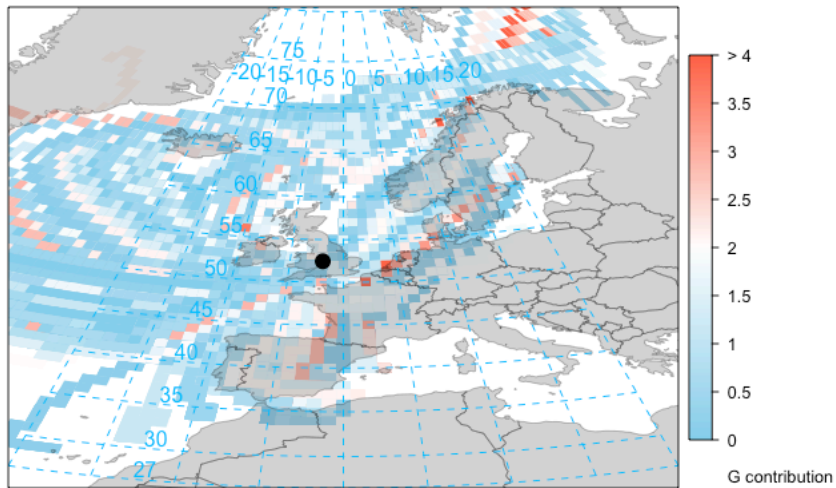
929

RG2



930

RG3



931

RG4

932 Figure 9: Average G contribution of the factors from the RG analysis for incoming air masses.

933 Higher contributions indicate better association of the given factor with the corresponding

934 air mass origin.